Infrastructure-Based Wireless Networks: Coverage and Percolation Properties

Sumanth Timmadasari[†], K. P. Naveen[*], and Srikrishna Bhashyam[§]
[†]Mediatek Bangalore Pvt. Ltd
[*]Department of Electrical Engineering, Indian Institute of Technology Tirupati, India
[§]Department of Electrical Engineering, Indian Institute of Technology Madras, India
Email: t.d.sumanth9630@gmail.com, naveenkp@iittp.ac.in, skrishna@ee.iitm.ac.in

***Abstract*—We present results from an extensive simulation study, conducted to understand the properties of coverage and percolation in infrastructure-based wireless networks that comprise sink and relay nodes. Specifically, we compute vacancy (complement of coverage) and percolation probabilities as functions of sink and relay node densities. Further, we identify that the vacancy probability in an alternate model that is motivated from traditional coverage processes, referred to as *independent-disc model*, constitutes a lower bound for the vacancy in the original infrastructure-based model. For the case of percolation, we identify a *threshold boundary* (in the space of sink-relay densities pair) where the percolation probability transits rapidly from 0 to 1 (i.e., from *no-percolation* to *full-percolation*).**

I. Introduction

Coverage and long-distance connectivity (percolation) crucially determine the QoS (Quality of Service) of a wireless network. The properties of these quantities (i.e., coverage and percolation) has been well understood for *all-infrastructure networks* (e.g., cellular, WiFi) where every node in the network is connected to an infrastructure backhaul [1]–[3]. For the case of coverage, its properties are also known for *infrastructure-less networks* where infrastructure support is available only at the edge of the network (e.g., ad hoc networks, wireless sensor networks) [4]. However, the behavior of coverage and percolation are less understood for *infrastructure-based networks* which generalizes the infrastructure-less setting by providing more infrastructure support into the core of network; alternatively, an infrastructure-based network can be thought as generalizing the all-infrastructure setting by incorporating relay nodes that can extend the network coverage by providing multi-hop paths to the infrastructure nodes.

Although there is work in the literature on infrastructure-based networks, this is however limited either to a one-dimensional setting (see [5] and references therein), or consider a restricted notion of connectivity model known as the Poisson AB model [6], [7]. In this work we conduct extensive simulations to understand the properties of coverage and percolation in infrastructure-based networks. Through our study we derive some valuable insights about the behavior of these quantities. Specifically, our main contributions are:

- **Coverage:** We obtain a lower-bound on vacancy by comparing our model with a traditional coverage processes model. We compute vacancies for other generalizations such as the hop-constrained model and the SINR model.
- **Percolation:** We generalize the algorithm in [8] to compute percolation probability for infrastructure-based networks. We identify a threshold boundary where rapid transition from no-percolation to full-percolation occurs.

The work of the second author was supported by an INSPIRE Faculty Award of the Department of Science and Technology, Government of India.

The paper is outlined as follows. In Section II we discuss the considered model in detail. Coverage properties are studied in Section III, while the percolation properties are presented in Section IV. We finally draw our conclusions in Section V.

II. System Model

We consider a wireless system comprising two types of nodes, namely, *sinks* and *relays* (infrastructure and infrastructure-less nodes, respectively). The sink nodes are assumed to be connected to an infrastructure backhaul, while the relay nodes are used to extend the network coverage by providing multi-hop paths to the sink nodes. The sink and relay nodes are distributed in $\mathcal{A}_L = \left[-\frac{L}{2}, \frac{L}{2}\right]^2 \subseteq \Re^2$ according to independent Poisson processes of intensities λ_S and λ_R, respectively. Note that, in case $L = \infty$ we simply have $\mathcal{A}_\infty = \Re^2$. Let $\lambda = \lambda_S + \lambda_R$ denote the aggregate node intensity while we use $\beta = \lambda_S/\lambda$ to represent the fraction of sink nodes in the network. Let r denote the transmission range of the nodes, both sink and relays. Thus, two nodes within a distance of r from each other can communicate directly, while nodes that are farther than distance r can (possibly) communicate via. multiple hops. In general, we introduce the following notion of connectivity (where, for simplicity, we refer to a node located at $x \in \mathcal{A}_L$ as *node-x*).

Definition 1 (h-connectivity): Nodes (or locations) x and y are said to be h-connected ($h \geq 0$) if there exists nodes (relay or sink) $z_1, \cdots, z_h$, not necessarily distinct, such that $\parallel x - z_1 \parallel \leq r$, $\parallel y - z_h \parallel \leq r$, and $\parallel z_i - z_{i-1} \parallel \leq r$ for $i = 2, \cdots, h$. In particular, x and y are 0-connected if $|x - y| \leq r$. We simply say x and y are *connected* if they are h-connected for some $h \geq 0$.

Thus, x and y are h-connected if they can communicate by multi-hopping via. at most h other nodes in the network. Also, note that since it is not necessary for the nodes $z_1, z_2, \cdots, z_h$ to be distinct, it follows that if x and y are h-connected then they are also ℓ-connected for all $\ell \geq h$.

Remark: The motivation for choosing a constant transmission range comes from the *SNR model*, according to which r represents the maximum distance (from a transmitting node) beyond which the SNR (Signal to Noise Ratio) falls below a threshold of Γ. Formally,

$$r = \sup\left\{d : \frac{Pd^{-\eta}}{N_0} \geq \Gamma\right\}$$

where P denotes the transmission power, $\eta > 2$ is the path-loss coefficient, and N_0 is the noise variance. The SNR model is applicable in scenarios where the transmissions from other nodes do not interfere with the intended signal at the receiver. We however note that a more realistic model is the SINR model where SINR (Signal to Interference plus Noise Ratio) is used to compute the transmission region around a node. For simplicity, we assume SNR model in our subsequent development; for the case of coverage, we however present results corresponding to the SINR case as well.

A. Coverage

We introduce a general notion of coverage by incorporating hop-counts into the defintion.

Definition 2 (h-Coverage): We say that a location $x \in \mathcal{A}_L$ is *h-covered* if there exists a sink node y such that (a node placed at) x and y are h-connected; otherwise we say that x is *h-vacant*. We say that x is *covered* if x is h-covered for some $h \geq 0$; otherwise x is said to be *vacant*.

Thus, if a location x is covered then, from x it is possible to communicate with some sink node in the network. In particular, we are interested in characterizing the probability that the origin $O = (0, 0)$ is covered, or alternatively that O is vacant. Formally, for a given λ and β, we introduce the notation $v_{\lambda,\beta}$ to denote the probability that O is vacant (*vacancy probability* or simply *vacancy*), i.e., $v_{\lambda,\beta} = \mathbb{P}(O \text{ is vacant})$. In general, we have $v_{\lambda,\beta,h} = \mathbb{P}(O \text{ is } h\text{-vacant})$.

Note that in the case of $\mathcal{A}_\infty$, $v_{\lambda,\beta}$ represents the fraction of vacant region in the network (this follows from ergodicity). The above conclusion is however not applicable for $\mathcal{A}_L$ (where L is finite) due to boundary effects. Nevertheless, for large L, $v_{\lambda,\beta}$ is a good approximation for the fraction of vacant region in the network.

In Section III we study the properties of the average vacancy $v_{\lambda,\beta}$ by varying λ and β. We derive a lower bound on $v_{\lambda,\beta}$ by drawing a comparison with an *independent-disk model*, studied in traditional coverage processes [9]. We also investigate the properties of vacancy in more general models such as the hop-constrained model (i.e., $v_{\lambda,\beta,h}$) and the SINR model.

B. Percolation

Percolation deals with the *macroscopic* property of whether long-distance communication is possible among far-off nodes in the network. This is in contrast to coverage which investigates the *microscopic* property of connectivity of the origin with the network.

Before proceeding further, for simplicity, we first introduce the following notation: Let $\mathcal{B}_L^{(L)}$ denote the left boundary of $\mathcal{A}_L$, i.e., $\mathcal{B}_L^{(L)} = \left\{-\frac{L}{2}\right\} \times \left[-\frac{L}{2}, \frac{L}{2}\right]$. The right, top and bottom boundaries of $\mathcal{A}_L$, denoted $\mathcal{B}_L^{(R)}$, $\mathcal{B}_L^{(T)}$ and $\mathcal{B}_L^{(B)}$, respectively, can be similarly defined. We then introduce the following notions of percolation:

Definition 3 (H, V, A and B Percolations):

- For a given λ_S, λ_R and $h \geq 0$, we say that *H-percolation occurs* (H for Horizontal) if there exists sink nodes $x_1, x_2, \cdots, x_n \in \mathcal{A}_L$ and locations $x_0 \in \mathcal{B}_L^{(L)}$ and $x_{n+1} \in \mathcal{B}_L^{(R)}$ such that x_i and x_{i+1} are h-connected for all $i = 0, 1, \cdots, n$. Thus, H-percolation occurs if and only if there exists a horizontal path of h-connected sink nodes that connects the left and right boundaries.
- Replacing the left and right boundaries in the above definition by the top and bottom boundaries ($\mathcal{B}_L^{(T)}$ and $\mathcal{B}_L^{(B)}$, respectively) we obtain the definition of V-percolation (V for vertical)
- we say that *A-percolation occurs* (A for Any) if either H-percolation or V-percolation occurs.
- In contrast to A-percolation, we say that *B-percolation occurs* (B for Both) if both H-percolation and V-percolation occurs.

Although the above definitions are applicable for a general $h \geq 0$, in this work, unless mentioned otherwise, we restrict our study of percolation to the case $h = 1$ (we defer the study of the general case to the future). Thus, for $h = 1$ the above definitions reduce to the setting where the successive sink nodes in the path $x_1, x_2, \cdots, x_n$ (including the locations x_0 and x_{n+1}) are connected by at most one relay node.

Now, *percolation probability* is simply defined as the probability that the respective percolation occurs. Formally, for $X \in \{H, V, A, B\}$ we define

$$p_X(\lambda_S, \lambda_R) \quad = \quad \mathbb{P}(X\text{-percolation occurs}). \qquad (1)$$

In Section IV we propose an algorithm to efficiently compute the above percolation probabilities as functions of (λ_S, λ_R); our algorithm is based on the technique proposed by Mertens and Moore in [8]. We then demonstrate a threshold boundary where sharp transition from *no-percolation* to *percolation* occurs.

III. Coverage Properties

The results from our simulation experiments are reported in Fig. 1; all plots in the figure correspond to $L = 10$ and $r = 1$. In Fig. 1(a) we plot $v_{\lambda,\beta}$ as a function of λ for different values of β. We immediately identify the following properties:

Property C1: $v_{\lambda,\beta}$ is decreasing in λ for a given β. In particular, $\lim_{\lambda\to\infty} v_{\lambda,\beta} = 0$.

Discussion: The above property can be understood directly from the definition of vacancy in Section II-A: As the node density increases the probability that O is connected to a sink node improves so that $v_{\lambda,\beta}$ decreases. It is possible to formally derive this result via. a coupling argument as follows. The process with node density λ_1 can be randomly thinned to reduce the density to $\lambda_2 < \lambda_1$ (note that random thinning

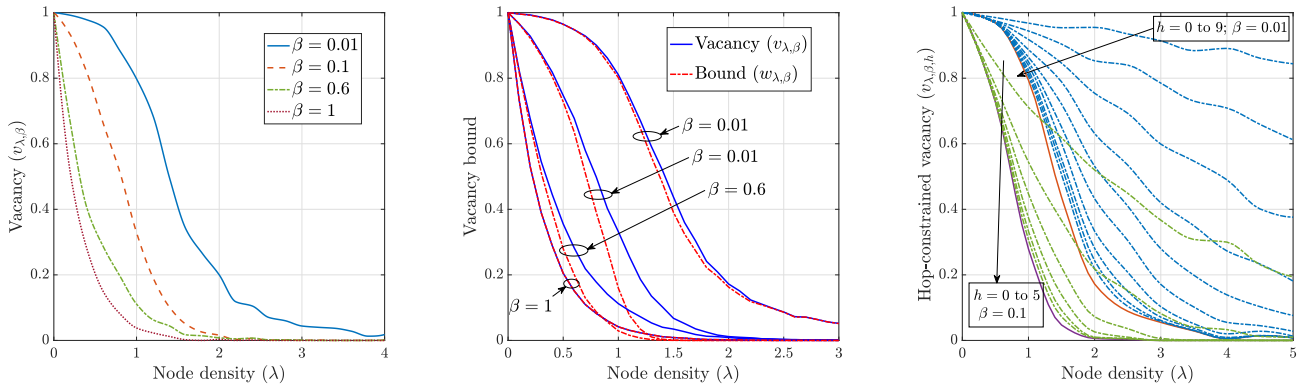

(a) (b) (c)

Fig. 1. (a) Vacancy vs. node density (b) Illustration of lower bound $w_{\lambda,\beta}$ obtained from the independent-disc model (c) Hop-constrained vacancy.

leaves β unchanged). Then, since vacancy in the first process implies vacancy in the second as well, we have $v_{\lambda_1,\beta} \leq v_{\lambda_2,\beta}$.

Property C2: $v_{\lambda,\beta}$ is decreasing in β for a given λ.

Discussion: Recall that β denotes the fraction of sink nodes in the network. Hence, a larger β implies a higher probability for O to be covered. Thus, $v_{\lambda,\beta}$ decreases with β. As in the discussion of Property C1, a formal proof can be derived via. a coupling argument.

A. Independent-disc Model

In Fig. 1(b) we demonstrate a lower bound on $v_{\lambda,\beta}$. In order to understand this result we need to introduce an alternate *independent-disc model*, and compare it with our model, referred to as the *dependent-disc model*. For this, we first modify Definition 1 to introduce a stringent notion of connectivity where only relays are used for multi-hopping:

Definition 4 (h-relay-connectivity): We say that x and y are *h-relay-connected* if there exists relay nodes $z_1, z_2, \cdots, z_h$, not necessarily distinct, such that $\| x - z_1 \| \leq r$, $\| y - z_h \| \leq r$, and $\| z_i - z_{i-1} \| \leq r$ for $i = 2, \cdots, h$. We simply say that x and y are *relay-connected* if they are h-relay-connected for some $h \geq 0$.

For each sink $x \in \mathcal{A}_L$ define

$$B_x = \Big\{ y \in \mathcal{A}_L : x \text{ and } y \text{ are relay-connected} \Big\}.$$

Thus, B_x denotes the set of locations (referred to as the *disc*) around x that are connected to x via. relay nodes.

Now, note that in our original model the collection of discs $\mathcal{B} = \{B_x : x \in \mathcal{A}_L \text{ is a sink}\}$ around all sink nodes in $\mathcal{A}_L$ are dependent since these are generated by the same realization of relay-node locations. Hence we refer to our model as the dependent-disc model. The above development yields the following alternate definition for vacancy: $v_{\lambda,\beta} = \mathbb{P}(O \notin \mathcal{B}_x \ \forall \text{ sink nodes } x \in \mathcal{A}_L)$.

In contrast to the above model, consider an alternate scenario where the discs are independent, while still being statistically identical to the discs in the original model. Formally, let $\overline{\mathcal{B}} = \{\overline{B}_x : x \in \mathcal{A}_L \text{ is a sink}\}$ denote a collection of independent discs such that $\overline{B}_x$ is statistically identical to B_x for each sink $x \in \mathcal{A}_L$. Then, the independent-disc model is obtained by replacing B_x by $\overline{B}_x$ for each sink $x \in \mathcal{A}_L$. One way to realize the independent-disc model is by obtaining discs $\overline{B}_x$ by generating independent Poisson process of relay-node locations for each sink node x. We use $w_{\lambda,\beta}$ to denote the vacancy in the independent-disk model, i.e., $w_{\lambda,\beta} = \mathbb{P}(O \notin \overline{\mathcal{B}}_x \ \forall \text{ sink nodes } x \in \mathcal{A}_L)$.

In Fig. 1(b) we have plotted $v_{\lambda,\beta}$ and $w_{\lambda,\beta}$ as functions of λ, for different values of β. We observe that $w_{\lambda,\beta}$ serves as a lower bound for $v_{\lambda,\beta}$, i.e., $w_{\lambda,\beta} \leq v_{\lambda,\beta}$. A proof of this result is known for one-dimensional networks in $\mathcal{A}_\infty$ [5]. We conjecture a similar result for the general case of two-dimensional networks in $\mathcal{A}_L$ (proof is deferred to the future):

Property C3: The vacancy $v_{\lambda,\beta}$ in the dependent-disc model is lower bounded by the vacancy $w_{\lambda,\beta}$ in the independent-disc model, i.e., $w_{\lambda,\beta} \leq v_{\lambda,\beta}$ for all (λ, β).

B. Hop-constrained Coverage

In Fig. 1(c) we show results from our study on hop-constrained vacancy. In particular, for $\beta = 0.01$ and $\beta = 0.1$ we plot $v_{\lambda,\beta,h}$ as a function of λ for different values of the hop constraint h. The solid curves in the figure correspond to the unconstrained vacancy $v_{\lambda,\beta}$. From Fig. 1(c) we identify the following property.

Property C4: For a fixed (λ, β), $v_{\lambda,\beta,h}$ is decreasing in h. Moreover, $\lim_{h\to\infty} v_{\lambda,\beta,h} = v_{\lambda,\beta}$.

Discussion: From Definition 1 we know that if x and y are h-connected then they are also ℓ-connected for $\ell \geq h$. In terms of vacancy of the origin, the above observation can be expressed as $\{O \text{ is } h\text{-vacant}\} \supset \{O \text{ is } \ell\text{-vacant}\}$, for $\ell \geq h$ which yields the first part of the above property. Second part follows by noting that $\cap_{h=0}^{\infty}\{O \text{ is } h\text{-vacant}\} = \{O \text{ is vacant}\}$.

From Fig. 1(c) we also observe that the value of h for which $v_{\lambda,\beta,h} \approx v_{\lambda,\beta}$ is larger for $\beta = 0.01$ than for $\beta = 0.1$ ($h = 9$ and $h = 5$, respectively). This is because a smaller β implies a sparser density of sink nodes, so that (on an average) a larger number of hops are required to reach a sink node from O.

C. The SINR Model

We have also conducted simulations to understand the properties of coverage in the more general SINR model [2], where

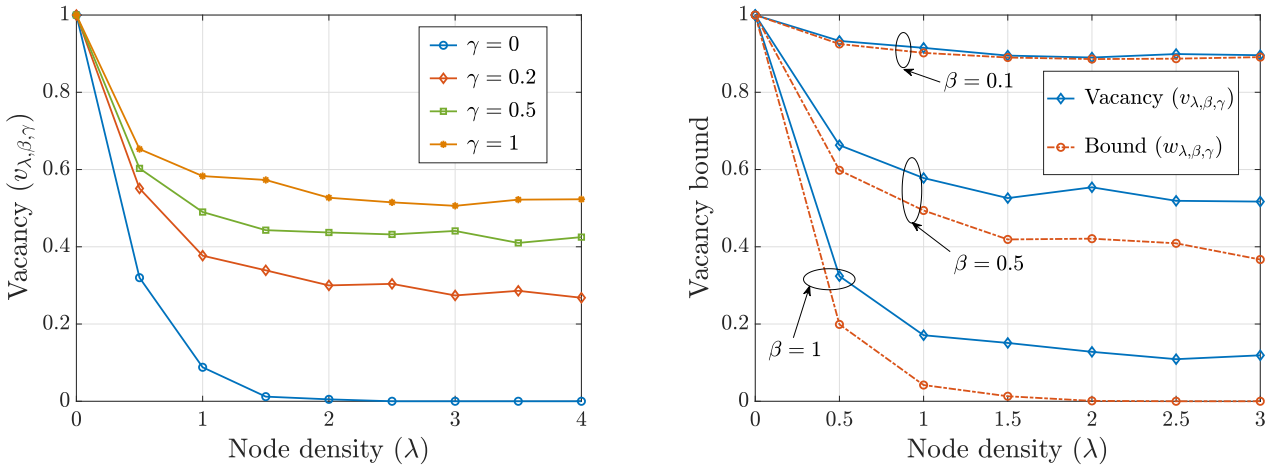

(a) (b)

Fig. 2. SINR model (a) Vacancy vs. node density (b) Lower bound on vacancy.

the interference due to other transmissions in the network are taken into account while establishing connectivity among the nodes. Formally, in the SINR model the power received at y due to transmission from x, denoted $P_{x,y}$, is given by (assuming P to be the transmit power of all nodes)

$$P_{x,y} = \frac{Pd_{x,y}^{-\eta}}{N_0 + \gamma \sum_{z \neq x,y} Pd_{z,y}^{-\eta}} \tag{2}$$

where the summation in the denomination is over all other nodes $z \in \mathcal{A}_L$, and thus represents the interference power. In the above expression, $d_{x,y}$ denotes the distance between x and y, N_0 is the noise variance, $\eta > 2$ is the path-loss exponent, and $\gamma \in [0,1]$ is a factor that determines the fraction of interference power that is received (see [2] for details). When $\gamma = 0$ expression (2) reduces to the earlier SNR model; in this sense the SINR model can be thought as a generalization.

We say that x *can communicate with* y if $P_{x,y} \geq \Gamma$ where Γ denotes the SINR constraint. However, for bidirectional communication to occur, it is necessary for x and y to communicate with each other. Thus, we say that x and y are connected if $P_{x,y} \geq \Gamma$ and $P_{y,x} \geq \Gamma$. With this definition of connectivity among two nodes, we extend the notion of coverage to the SINR model by saying that O is covered if there exists a path to some sink node in $\mathcal{A}_L$; otherwise O is said to be vacant (for simplicity, we are not concerned about the number of hops taken). Analogously, we let $v_{\lambda,\beta,\gamma}$ to denote the probability that O is vacant.

In Fig. 2(a) we depict $v_{\lambda,\beta,\gamma}$ as a function of λ for different value of γ. The plots correspond to $\beta = 0.5$, while the model parameter values are fixed at $L = 10$, $P = 2$, $\eta = 4$, $N_0 = 5$, and $\Gamma = 0.4$. As before, we see that $v_{\lambda,\beta,\gamma}$ decreases with λ. However, interestingly for $\gamma > 0$ we find that $v_{\lambda,\beta,\gamma}$ converges to a non-zero value as λ increase. This is possibly because of the increase in interference, which reduces the connectivity among nodes in the network. Thus, unlike in the SNR model, here it is not possible to achieve 100% by increasing λ.

Finally, we also compute $w_{\lambda,\beta,\gamma}$ which denotes the vacancy created in the independent-disc model (analogous to the one discussed in Section III-A). In Fig. 2(b) we compare $v_{\lambda,\beta,\gamma}$ against $w_{\lambda,\beta,\gamma}$ for different values of β; we have fixed $\gamma = 1$ which represents the scenario where the interference power is maximum. As for the SNR model, we find that $w_{\lambda,\beta,\gamma}$ constitutes a lower bound for $v_{\lambda,\beta,\gamma}$.

IV. Percolation Properties

First, recalling Definition 3 and the expression for percolation probability from (1), we immediately identify the following properties:

Property P1: $p_H(\lambda_S, \lambda_R) = p_V(\lambda_S, \lambda_R)$.

Property P2: $p_B(\lambda_S, \lambda_R) \leq p_H(\lambda_S, \lambda_R) \leq p_A(\lambda_S, \lambda_R)$.

Property P1 simply follows because the horizontal and vertical directions are statistically identical. To deduce Property P2, note that $\{B$-percolation occurs$\} \subset \{H$-percolation occurs$\} \subset \{A$-percolation occurs$\}$.

We next proceed to numerically-compute the various percolation probabilities. For this, we employ the technique proposed by Mertens and Moore in [8]. In fact, we generalize their approach to the current setting where nodes of two types (i.e., sink and relays) are involved (in contrast, the original procedure in [8] is applicable for a network comprising all sink nodes). The details are discussed in the following.

A. Computation of Percolation Probabilities

In Algorithm 1 we present the simulation procedure to compute the minimum number of nodes required for percolation to occur. The output from Algorithm 1 will be used to compute percolation probabilities.

The algorithm begins by adding a new node into the network. The added node is designated either a sink or a relay with probability β and $(1-\beta)$, respectively. The network is then checked for whether X-percolation occurs (for $X = A, H, B$). Note that, we do not explicitly report the occurrence of V-percolation as it is statistically identical to H-percolation

(Property P1). Also, from Property P2 we know that A, H and B-percolations occur in the same order as mentioned. Hence, it is not necessary to check for H-percolation if A-percolation has not occurred, and so on (for simplicity of exposition, we have not embedded this observation into the pseudocode of Algorithm 1). To efficiently check for percolation, we use the *union-find algorithm* [8] which keeps track of the clusters in the network, while simultaneously checking for horizontal and vertical crossing of these clusters.

When X-percolation occurs (indicated by $X_{FLAG} = 1$), the number of sink and relay nodes present in the network at that instant are reported in the matrix N_X. The procedure (of adding a new node and checking for the occurrence of the various percolations) is continued until all three percolations occur, at which instant the current simulation run ends. The algorithm conducts similar simulation experiment for a total of N iterations. Thus, at the end of N iterations, the value $N_X(i,j)$ (for any $(i,j) \in \mathbb{N}^2$) represents the total number of times X-percolation occurred with i sink and j relay nodes in the network. The output $F_X(n_S, n_R)$ (for $(n_S, n_R) \in \mathbb{N}^2$) is thus an estimate of the probability that X-percolation occurs whenever the network contains n_S sink and n_R relay nodes.

Define $\Lambda_\beta = \left\{(\lambda_S, \lambda_R) : \frac{\lambda_S}{\lambda_S+\lambda_R} = \beta\right\}$. Then, for any $(\lambda_S, \lambda_R) \in \Lambda_\beta$, various percolation probabilities can be estimated numerically using the output from Algorithm 1 as follows: for $X \in \{A, H, B\}$ we have

$$p_X(\lambda_S, \lambda_R) = \sum_{n_S, n_R=0}^{\infty} \frac{(\lambda_S L^2)^{n_S}}{n_S!} \frac{(\lambda_R L^2)^{n_R}}{n_R!} e^{-(\lambda_S+\lambda_R)L^2} F_X(n_S, n_R). \quad (3)$$

Note that, for $\beta = 1$ (in which case $\lambda_R = 0$) the above procedure reduces to the *all-infrastructure* setting considered in [8] where each node is a sink, so that percolation occurs whenever there is a horizontal/vertical path of sink nodes crossing the boundaries.

Algorithm 1: Percolation Probability Computation

Input: L, r, β, and N;
Initialization:
    $N_X(i,j) = 0 \ \forall (i,j) \in \mathbb{N}^2$ and $X \in \{A, H, B\}$;
for $i = 1 : N$ **do**
    $i_S = i_R = 0$;
    $X_{FLAG} = 0$ for $X \in \{A, H, B\}$;
    while $B_{FLAG} = 0$ **do**
        Place a new node randomly in $\mathcal{A}_L$;
        $X \sim Ber(\beta)$;
        if *X=1* **then**
            Designate the new node as sink;
            $i_S = i_S + 1$;
        else
            Designate the new node as relay;
            $i_R = i_R + 1$;
        end
        for $X = A, H, B$ **do**
            % Check for X-percolation
            if $X_{FLAG} == 0$ *& X-percolation occurs* **then**
                $N_X(i_S, i_R) = N_X(i_S, i_R) + 1$;
                $X_{FLAG} = 1$
            end
        end
    end
end
Output: $F_X(n_S, n_R) = \sum_{i=0}^{n_S} \sum_{j=0}^{n_R} \frac{N_X(i,j)}{N}$ for all $(n_S, n_R) \in \mathbb{N}^2$ and $X \in \{A, H, B\}$

B. Simulation Results

We first consider the case $\beta = 1$, where the percolation probabilities $p_X(\lambda_S, 0)$ $(X \in \{A, H, B\})$ are simply functions of the sink density λ_S. In Fig. 3(a), 3(b) and 3(c) we plot A, H and B-percolation probabilities, respectively, as functions of sink density λ_S for different values of L. For simplicity, we have fixed the transmission radius $r = 1$. From the plots in Fig. 3 we identify percolation thresholds, $\lambda^{(X)}$ $(X \in \{A, H, B\})$, around which transition from *no-percolation* to *percolation* occurs. We also notice that the steepness of the curves around these thresholds increases with

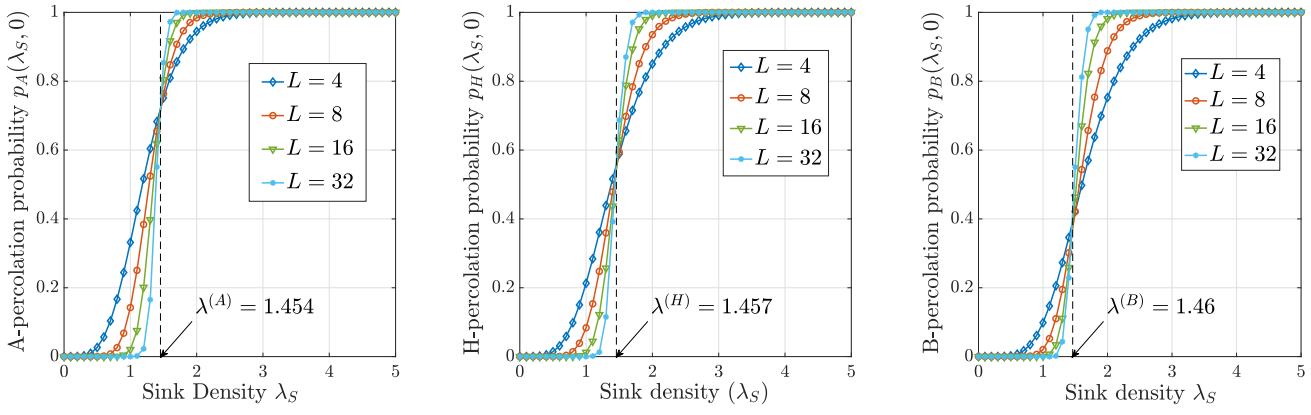

(a) (b) (c)

Fig. 3. Illustration of the percolation threshold $\lambda^{(X)}$ for the case where $\beta = 1$ (a) Any percolation (b) Horizontal percolation (c) Both percolation.

L, implying that the *ideal percolation behaviour* (of strictly 0 and 1 probability of percolation, respectively, below and above a threshold) is approached as L increases. We note this result as a property:

Property P3: For large L, there exists a threshold $\lambda^{(X)}$ ($X \in \{A, H, B\}$) such that

$$p_X(\lambda_S, 0) \approx \begin{cases} 0 & \text{if } \lambda_S < \lambda^{(X)} \\ 1 & \text{if } \lambda_S > \lambda^{(X)}. \end{cases} \quad (4)$$

We also see that the thresholds in Fig. 3 satisfy $\lambda^{(A)} \leq \lambda^{(H)} \leq \lambda^{(B)}$ which is in accordance with the observation made in Property P2. However, the difference in the values of these thresholds are negligable; indeed, in $\mathcal{A}_\infty = \Re^2$ the different notions of percolations (i.e., H, V, A and B-percolations) coincide, in the sense that an unbounded cluster of connected nodes in $\Re^2$ extends in all directions. Thus, as L increases we expect these different thresholds to coincide.

We next proceed to study the general case of infrastructure-based network where both sink and relay nodes are present. We fix $L = 16$ and (as before) $r = 1$. In Fig. 4 we depict H-percolation probability[1] $p_H(\lambda_S, \lambda_R)$ as a heat-map obtained by varying λ_S and λ_R. Analogous to the earlier ($\beta = 1$) case where percolation was characterized by a threshold, here we see that there exists a boundary beyond which percolation probability starts transiting from 0 to 1. In Fig. 4 we have (approximately marked and) shown using solid line a 60% threshold-boundary where the percolation probability starts exceeding 0.6; similarly, the dashed line indicates an 85% threshold-boundary. We expect the transitions to become steeper as the value of L is increased, so that for a large L we obtain a well defined percolation boundary where the percolation probability jumps from 0 to 1. Based on the observations made from Fig. 4, we infer the following property about the percolation boundary.

Property P4: For large L, there exists thresholds $\lambda_1^{(H)} < \lambda_2^{(H)}$ on sink density, and $\mu^{(H)}$ on relay density such that

- For $\lambda_S < \lambda_1^{(H)}$ the network does not percolate (even for any large value of relay node density). Thus, relays cannot cause percolation to occur when the sink density is below the critical threshold of $\lambda_1^{(H)}$
- For $\lambda_S > \lambda_2^{(H)}$ the network percolates (even when the relay density is 0). Thus, relays are not necessary for percolation to occur when the sink density is above the critical threshold of $\lambda_2^{(H)}$.
- For $\lambda_1^{(H)} < \lambda_S < \lambda_2^{(H)}$, percolation occurs if and only if $\lambda_R > \mu^{(H)}(\lambda_2^{(H)} - \lambda_S)/(\lambda_2^{(H)} - \lambda_1^{(H)})$. Thus, in this regime, along with the sink nodes a critical density of relay nodes are required to ensure percolation.

See Fig. 4 for an illustration of the above thresholds. Finally, a careful investigation of Fig. 3(b) and Fig. 4 suggests that $\lambda_2^{(H)} = \lambda^{(H)}$; this should not be surprising as the plot in Fig. 3(b) is identical to the data along $\lambda_R = 0$ line of Fig. 4.

[1]Due to space constraint we restrict our attention to H-percolation hereafter. However, we note that the properties of A and B-percolations are very similar to those exhibited by H-percolation (as was the case with the all-infrastructure setting studied in Fig. 3).

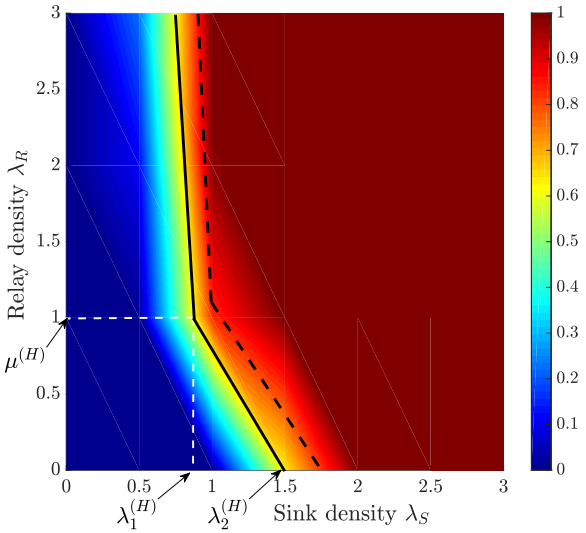

Fig. 4. Heat-map of the percolation probability $p_H(\lambda_S, \lambda_R)$.

V. Conclusion

Through our simulation work we established some valuable properties of coverage and percolation in infrastructure-based networks. Specifically, we identified that the vacancy probability is lower bounded by its counterpart in an independent-disc model studied in coverage processes. For the SINR model, due to interference the vacancy probability does not reduce to zero as the node density increases (which is in contrast to that observed for the SNR model). For the case of percolation, we identified a boundary where the percolation probability undergoes a sharp transition from 0 to 1. We finally characterized the structure of the percolation boundary by using certain thresholds on sink and relay node densities.

References

[1] J. G. Andrews, F. Baccelli, and R. K. Ganti, "A Tractable Approach to Coverage and Rate in Cellular Networks," *IEEE Transactions on Communications*, vol. 59, no. 11, pp. 3122–3134, November 2011.

[2] O. Dousse, M. Franceschetti, N. Macris, R. Meester, and P. Thiran, "Percolation in the Signal to Interference Ratio graph," *Journal of Applied Probability*, vol. 43, no. 2, p. 552?562, 2006.

[3] L. Booth, J. Bruck, M. Franceschetti, and R. Meester, "Covering Algorithms, Continuum Percolation and the Geometry of Wireless Networks," *The Annals of Applied Probability*, vol. 13, no. 2, pp. 722–741, 05 2003.

[4] D. Miorandi, E. Altman, and G. Alfano, "The Impact of Channel Randomness on Coverage and Connectivity of Ad Hoc and Sensor Networks," *IEEE Transactions on Wireless Communications*, vol. 7, no. 3, pp. 1062–1072, March 2008.

[5] K. P. Naveen and A. Kumar, "Coverage Properties of One-Dimensional Infrastructure-Based Wireless Networks," in *Proceedings of the 19th ACM International Conference on Modeling, Analysis and Simulation of Wireless and Mobile Systems*. NY, USA: ACM, 2016, pp. 348–357.

[6] S. K. Iyer and D. Yogeshwaran, "Percolation and Connectivity in AB Random Geometric Graphs," *Advances in Applied Probability*, vol. 44, no. 1, pp. 21–41, 03 2012.

[7] M. D. Penrose, "Continuum AB Percolation and AB Random Geometric Graphs," *Journal of Applied Probability*, vol. 51A, pp. 333–344, 12 2014.

[8] S. Mertens and C. Moore, "Continuum Percolation Thresholds in Two Dimensions," *Physical Review E*, vol. 86, Dec 2012.

[9] P. Hall, *Introduction to the Theory of Coverage Processes*, ser. Wiley Series in Probability and Mathematical Statistics. NY: Wiley, 1988.